研究課題別評価

1 研究課題名:

High-frequency electron-spin manipulation in semiconductor artificial atoms and molecules

2 研究者氏名:

Wilfred G. van der Wiel

3 研究のねらい:

The aim of the project is high-frequency (GHz) electron-spin manipulation in semiconductor few-electron quantum dots. The main motivation of this proposal is formed by the possible application of electron spins as basic building blocks for quantum logic.

One concrete aim is to rotate a single-electron spin in a few-electron quantum by means of a locally generated electron spin resonance (ESR) field. A key experiment that still needs to be done is the determination of the single-electron spin decoherence time T_2 in a semiconductor environment. The next logical step after studying single dots is to look at double dot systems. The entanglement of two electron spins using tunnel-coupled quantum dots is of great importance for the realization of the XOR (or controlled-NOT) gate operation.

4 研究成果:

4.1. Few-electron quantum dot devices for single electron spin resonance

We have fabricated vertical few-electron quantum dot (QD) devices with an integrated high-frequency line to generate an ac magnetic field in the vicinity of the QD [1,2]. This ac magnetic field is intended for realizing single electron spin resonance (ESR) and measuring the single-electron coherence time T_2. The effective g-factor in our GaAs dot is derived and microwave experiments show the importance of photon assisted tunneling (PAT) and pumping.

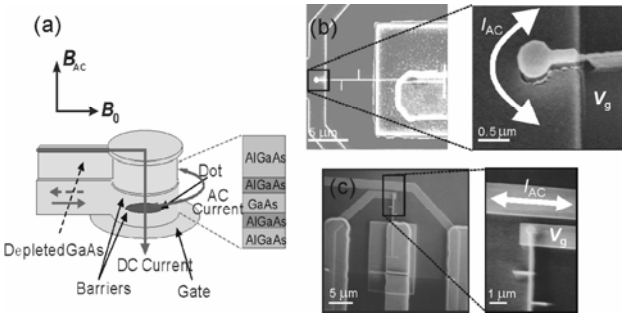

FIGURE 1. (a) Schematic of a vertical quantum dot (VQD) with a ring gate used for generating an ac magnetic field B_{ac}. The device is positioned in a static magnetic field B_0 parallel to the dot plane. (b) Scanning electron microscope (SEM) pictures of a VQD device with a local ac magnetic field generator. In the "combination type" a Ti/Au gate electrode is used for applying both a DC voltage and an ac current. (c) SEM pictures of a VQD device with a separate local ac magnetic field generator. In the "separate wire type" a Ti/Au wire is fabricated in the vicinity (~1 μm) of the dot.

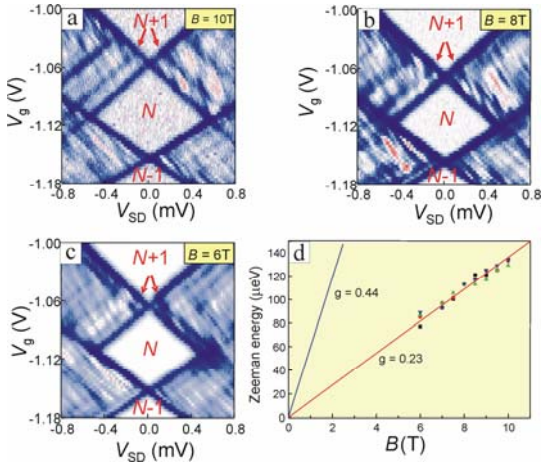

FIGURE 2. Plots of the differential conductance dI/dV vs. gate voltage V_g and source-drain voltage V_{sd} for three different parallel magnetic fields, B = 10 T (a), 8 T (b), and 6 T (c). The B-evolution of a Zeeman split state (indicated by arrows) is clearly observed. (d) Zeeman energy as a function of B. The Zeeman energy cannot be resolved for B < 6 T. From the linear fit to the data (red line) $|g_{dot}| = 0.23 \pm 0.02$ is derived. The Zeeman energy in bulk GaAs ($|g_{GaAs}| = 0.44$) is plotted for comparison. The different symbols correspond to different positions in the Coulomb diamond where the Zeeman splitting has been evaluated.

Examples of our ESR devices are shown in Fig. 1. Ideally, a single electron is confined in the QD and its discrete orbital energy level is Zeeman split due to a static magnetic field B_0 by $\Delta E_Z = g_{dot}\mu_B B_0$ with g_{dot} the g-factor in the dot and μ_B the Bohr magneton. A microwave magnetic field, B_{ac}, in a plane perpendicular to B_0 and in resonance with the precession rate, causes coherent oscillations between the states $|\uparrow\rangle$ and $|\downarrow\rangle$ (electron spin resonance: ESR). The rotation frequency, or Rabi frequency, is proportional to the strength of B_{ac}: $f_{Rabi} = g_{dot}\mu_B B_{ac}/h$. The field B_{ac} is generated by driving an ac current Iac through a microstripline in the vicinity of the QD. The Larmor precession and the B_{ac}-induced Rabi oscillations offer two perpendicular axes of rotation, enabling in principle any desired qubit rotation.

Since g_{dot} is expected to differ significantly from the value in bulk GaAs we first independently determined g_{dot}, using excited state spectroscopy, as shown in Fig. 2. The Zeeman energy is derived for a series of magnetic fields from the energy spacing between the ground state and the Zeeman excited state (indicated by red arrows). We derive $|g_{dot}| = 0.23 \pm 0.02$, which is smaller than that of bulk GaAs ($|g_{GaAs}| = 0.44$), probably due to the effect of electron confinement and the influence of the $Al_{0.3}Ga_{0.7}As$ barriers (bulk g-factor +0.4).

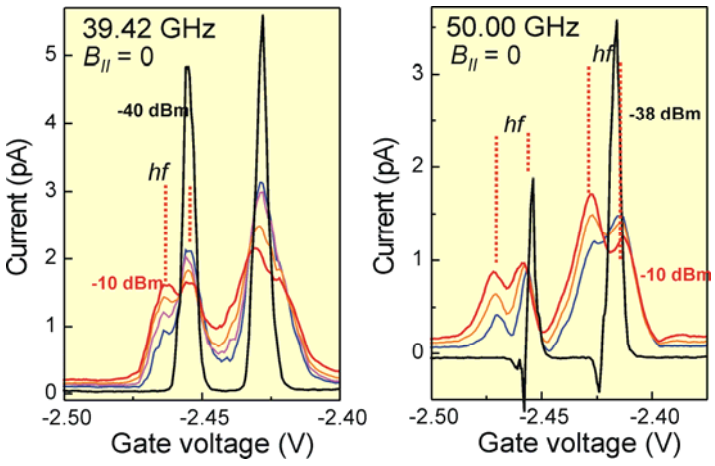

FIGURE 3. I-V_g plots at B = 0 for microwave powers from −40 to −10 dBm, f = 39.42 GHz (a) and from −38 to −10 dBm, f = 50 GHz (b). Satellite peaks ascribed to photon assisted tunneling are indicated.

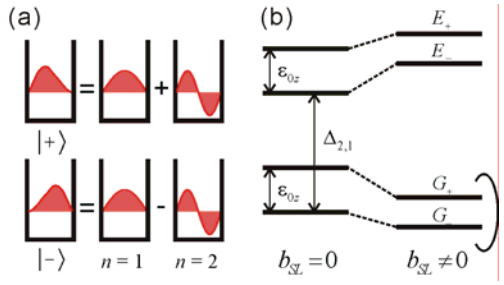

FIGURE 4. (a) Schematic hybridization of multiple orbital states. (b) Energy spectrum of a quantum dot (QD) with two orbital levels (level spacing $\Delta_{2,1}$) and Zeeman energy ε_{0z} with/without a magnetic field gradient b_{SL}. The lowest levels, $|G_{\pm}\rangle$, constitute a qubit. $|E_{\pm}\rangle$ are excited states.

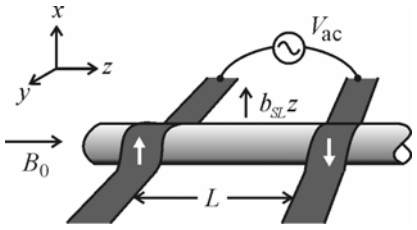

FIGURE 5. Model of the 1D QD in a slanting Zeeman field. Ferromagnetic gate electrodes (dark grey) are located at either end of the dot and are magnetically polarized in the plus/minus x-direction, creating a magnetic field gradient b_{SL}. A uniform magnetic field B_0 is applied in the z-direction. The spin in the dot is controlled by applying an oscillating voltage V_{ac} between the two gates.

Our microwave results (Fig. 4) indicate that instead of generating only an AC magnetic field, we also create a significant AC electric field near the dot. We have not been able to confirm ESR in our system, hampered by the spurious electric ac field. Our results confirm that microwave signals up to 50 GHz reach the sample, but also indicate that we have to reduce the AC voltage generated in the dot and possibly also the heating of the sample.

As an alternative for the above strategy, we have described a general concept for realizing a solid-state quantum two-level system (Fig.4), based on a single electron in a quantum dot (Fig.5), which combines ease of manipulation with long coherence times [3]. An ac voltage is applied to let an electron in a QD oscillate under a *static* slanting Zeeman field. This effectively provides the electron spin with the necessary time-dependent magnetic field. Note the analogy with the Stern-Gerlach experiment, where the spin and orbital degrees of freedom are coupled by employing an inhomogenous magnetic field. A robust single pseudo-spin system is obtained that can be controlled by voltage only, without the need for an external time-dependent magnetic field or spin-orbit coupling. This unique and important feature is expected to considerably facilitate experimental realization of qubits based on single electrons. It is shown that both single qubit rotations and the C-NOT operation can be realized, thereby providing a universal set of gates for quantum computation. Using this approach it is also possible to determine the intrinsic single electron spin coherence time in the system.

4.2. Electron–phonon Coupling in a Double Quantum Dot

Electron–phonon coupling often leads to dissipation and decoherence problems in nanoelectronic devices. The decoherence in a tunable two-level quantum system (qubit), such as a double quantum dot (DQD) [4], is of particular interest in the recent light of quantum computation and information. In analogy to quantum states in natural atoms – which dominantly couple to, and are successfully controlled by photons – the electronic states in solid state systems may be controlled by phonons, taking advantage of the strong electron–phonon coupling. We have observed non-adiabatic transport through a double quantum dot under irradiation of surface acoustic waves generated on-chip [5]. At low excitation powers, absorption and emission of single and multiple phonons is observed. At higher power, sequential phonon assisted tunneling processes excite the double dot in a highly non-equilibrium state. The present system is attractive for studying electron–phonon interaction with piezoelectric coupling.

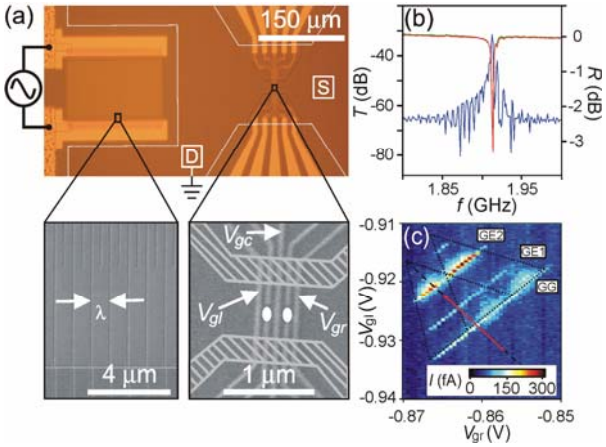

FIGURE 6. (a) Picture of the device with interdigital transducer (IDT, left) and double quantum dot (DQD, right). The source (S) and drain (D) reservoirs are indicated. The IDT-DQD distance is 227.5 μm. In the scanning electron micrograph (SEM) of the IDT, the electrodes, separated by λ = 1.4 μm, are visible. In the hatched regions of the DQD SEM the 2DEG is depleted by dry etching. The position of the dots is indicated by white dots. (b) Transmission T (blue curve) and reflection R (red and greencurves) at room temperature of two IDTs similar to the one used in the experiments, separated by a distance of 455 μm. A peak in T and a dip in R are visible at 1.92 GHz. (c) Color scale plot of the DQD current vs. gate voltages V_{gl} and V_{gr} at source drain voltage V_{SD} = 500 μV without SAWs. The dual gate sweep direction for the SAW experiments is indicated by the red arrow.

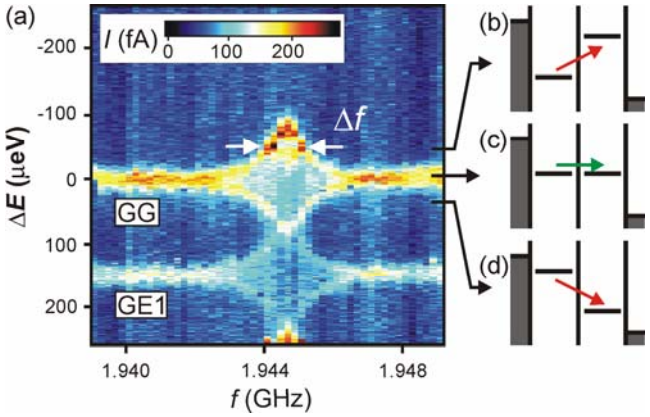

FIGURE 7. (a) Color scale plot of the DQD current versus ground state level spacing ΔE and microwave frequency f applied to the IDT (-40 dBm microwave power). V_{gl} and V_{gr} are swept along the red arrow indicated in Fig. 1(c). The current at ΔE=0 and 150 μeV corresponds to resonant tunneling through the ground states (GG), and through the left ground state and an excited state in the right dot (GE1), respectively. A clear resonance is observed at 1.9446 GHz (Δf = 1.4 MHz), corresponding to the IDT resonance frequency. The inelastic current is due to absorption and emission of SAW phonons, as schematically depicted in the energy diagrams (b) and (d), respectively. The energy diagram for elastic resonant tunneling is shown in (c).

Our device is described in Fig. 6. Figure 6(c) shows the single-electron tunneling current through the DQD versus gate voltages V_{gl} and V_{gr} with a large bias voltage of 500 μV with no microwave power (P = 0) applied to the IDT. When microwaves are applied to the IDT, we observe significant broadening and splitting of the resonant tunneling peaks only at the IDT resonant frequency, f_{SAW} = 1.9446 GHz, as seen in the frequency dependence of the current spectrum in Fig. 7(a). The resonance frequency corresponds very well to that of the GaAs reference sample (1.92 GHz) of Fig. 6(b).

The microwave power dependence of the current spectra is presented in Fig. 8(a). The peak splitting clearly increases with microwave power P. In Fig. 8(d) the splitting is plotted (black dots) as function of the amplitude of the microwave voltage applied to the IDT, V_{IDT}, confirming the linear dependence. The non-adiabatic calculation in Fig. 8(c) shows clear additional structure in between the split peaks. This structure originates from the phonon satellite peaks that should be individually resolvable at $\Delta E = nhf_{SAW}$ if the peak width is smaller than the phonon energy. In our case, however, the peak width exceeds hf_{SAW} (but is less than $2hf_{SAW}$). We actually find good agreement between the calculated current spectra and the experimental data (including the inter-peak fine

structure) at finite microwave power as shown in Fig. 8(b), where we have applied the α–PdBm conversion derived in Fig. 8(d). Our data thus reveal clear quantum behavior, even when we cannot resolve individual phonon satellites. Quantum behavior is also observed in multiple excitation processes between excited states at higher power [Fig. 8(e)].

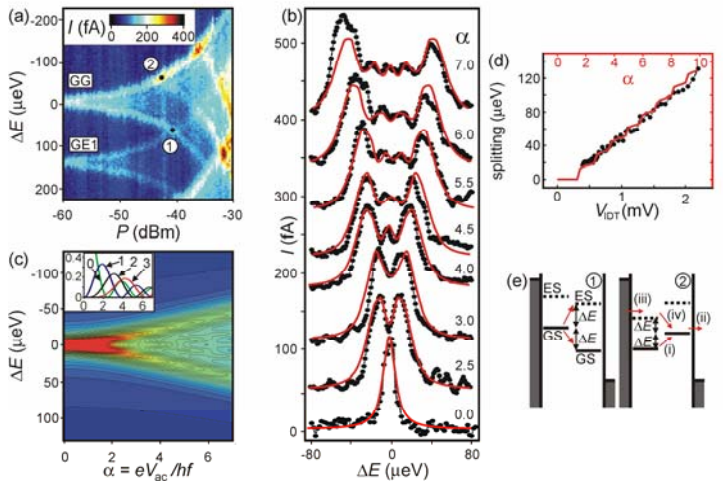

FIGURE 8. (a) Color scale plot of the DQD current versus ΔE and microwave power P, at f_{SAW}= 1.9446 GHz, for the same transitions as in Fig. 2. (b) Experimental (black dots) and calculated (red curves) current spectra for different microwave powers, extracted from (a) and (c), respectively. The experimental microwave power incident on the IDT is converted to normalized potential amplitude α using (d). The current height of the calculated spectra is fitted to the experimental data. (c) Calculated DQD current versus ΔE and α in the non-adiabatic limit, as explained in the text. Inset: squared Bessel functions $J_n^2(\alpha)$ for n = 0,1,2 and 3. (d) Splitting of the current peaks as function of the amplitude of the microwave voltage V_{IDT} applied to the IDT for the experimental data (black data points and axes), and current peak splitting derived from the calculated spectra in (c) as function of α (red curve and axes). By matching the experimental and calculated curves, the conversion between P and α is found. (e) Schematic energy level diagrams for the positions 1 and 2 indicated in (a).

The current spectra reflect the amplitude of the local piezoelectric potential. The lowest power at which we can resolve peak splitting is −58 dBm, corresponding to V_{pe} = 24 μV, which is several orders of magnitude smaller than the power used to induce dynamical quantum dots and to induce lattice displacements measurable by optical interferometry. We find that the DQD can be employed as a very sensitive SAW detector and is promising for studying electron–phonon interaction.

References

[1] T. Kodera, W.G. van der Wiel, K. Ono, S. Sasaki, T. Fujisawa and S. Tarucha, Physica E **22**, 518 (2004).

[2] T. Kodera, W.G. van der Wiel, T. Maruyama, Y. Hirayama and S. Tarucha, in *Realizing controllable quantum states*, H. Takayanagi, J. Nitta (eds.), pp. 445–450, World Scientific Publishing, Singapore (2005).

[3] Y. Tokura, W.G. van der Wiel, T. Obata and S. Tarucha, Phys. Rev. Lett., in press; cond-mat/0510411 (2005).

[4] W. G. van der Wiel, S. De Franceschi, J. M. Elzerman T. Fujisawa, S. Tarucha and L. P. Kouwenhoven, Rev. Mod. Phys. **75**, 1 (2003).

[5] W.J.M. Naber, T. Fujisawa, H.W. Liu and W.G. van der Wiel, submitted to Physical Review Letters; cond-mat/0601158 (2006).

5 自己評価:

The original goal of realzing single-electron electron spin resonance (ESR) has turned out to be extremely hard. The main problem is formed by spurious ac electric fields that obscure a possible ESR signal. Similar kind of problems have been decribed by groups at Harvard University and Delft University of Technology, where also attempts have been made to realize single-electron ESR. Motivated by the practical problems we came across, we have started working on a pulse-and-probe scheme that should, in principle, be able to cope with the problems. In addition, we have developed an alternative scheme based on a single electron in a slanting magnetic field, as discussed above. This work has resulted in a publication in Physical Review Letters. Experimental work on the realization of single-electron ESR will continue, based on the ideas developed.

As far as double quantum dots are concerned, we have made important progress in studying electron–phonon interaction in a potential two-qubit system. The work was recently submitted to Physical Review Letters and is expected to function as a stimulus for research on controlled electron–phonon interaction.

6　研究総括の見解：

半導体中の電子スピン状態を自由に制御することは将来の量子情報処理への有力な方法として期待されている。本研究は少数の電子を閉じ込める微細な量子ドットを対象に、電子スピン共鳴(ESR)の手法を用いて制御することを目的に行った実験的研究である。主要な研究成果として次の 3 点を挙げることが出来る。第 1 に量子井戸結晶成長と微細加工法を用いて作成した柱状量子ドット素子を自作し、磁気測定を行うことにより、g因子が 3 次元状態と異なること(g=0.33)を明らかにしたこと；第 2 に当初計画したESR法によるスピン制御は、残留交流電場の存在のために正しい動作が出来ないことが明らかとなり、これに代わるものとして傾斜磁場を用いた新しい制御法を考案し、理論予測を行ったこと；第 3 にスピン状態のコヒーレンス時間(T_2時間)を支配する電子―フォノン相互作用を直接に明らかにするために、2 重トンネル量子井戸構造の素子に表面波超音波を照射し、フォノンに助けられたトンネル効果の直接観察に初めて成功しフォノン結合の強さを推定したこと、である。

研究成果は 9 篇の原著論文、1 篇の解説論文、8 件の招待講演等で公表している。特に半導体量子ドット構造を用いた電子制御の一連の研究をまとめた総合報告(Rev. Mod. Phys.誌)は約 150 回も引用され、また量子情報に関するゴードン会議の座長を勤めるなど、当分野の第一線の研究者として認知されている。本研究の結果は電子スピンを一つずつ制御するための基礎となる重要な知見であり、当初の予想とは異なるものの全体として予想を超える成果と判断する。

7　主な論文等：

論文

05. **Surface acoustic wave induced transport in a double quantum dot**
W.J.M. Naber, T. Fujisawa, H.W. Liu and W.G. van der Wiel
Physical Review Letters, *in press*; cond-mat/0601158 (2006).

04. **Coherent single electron spin control in a slanting Zeeman field**
Y. Tokura, W.G. van der Wiel, T. Obata and S. Tarucha
Phys. Rev. Lett. **96**, 047202 (2006).

03. **Fabrication and characterization of quantum dot single electronspin resonance devices**
T. Kodera, W.G. van der Wiel, T. Maruyama, Y. Hirayama and
S. Tarucha, in *Realizing controllable quantum states*, H. Takayanagi, J. Nitta (eds.), pp. 445–450, World Scientific Publishing, Singapore (2005).

02. **Fabrication and characterization of quantum dot single electronspin resonance devices**
T. Kodera, W.G. van der Wiel, T. Maruyama, Y. Hirayama and
S. Tarucha, in *Realizing controllable quantum states*, H. Takayanagi, J. Nitta (eds.), pp. 445–450, World Scientific Publishing, Singapore (2005).

01. **Electron transport through double quantum dots**
W.G. van der Wiel, S. De Franceschi, J.M. Elzerman, T. Fujisawa,
S. Tarucha and L.P. Kouwenhoven
Rev. Mod. Phys. **75**, 1 (2003). [163 citations]

特許：なし
受賞：なし

招待講演等

05. **Electron charge and spin in semiconductor quantum dots (plenary)**
37th Conference of the European Group for Atomic Systems (EGAS37), Dublin, Ireland, 3-6 August 2005

04. **Electron spin qubits in semiconductor quantum dots (invited seminar)**
Stanford University, USA, 15 November 2004

03. **Quantum computation using electron spins in semiconductor quantum dots**
42nd Kaya Conference, Zaou, Japan, 22-25 August 2004

02. **Electron transport experiments in semiconductor quantum dots**
International Summer School for Young Researchers on Quantum Transport in Mesoscopic Scale & Low Dimensions, Kashiwa, Japan, 13-21 August 2003

01. **Microwave electron spin manipulation in semiconductor artificial atoms and molecules**
PASPS8, The 8th Symposium on the Physics and Application of Spin Related Phenomena in Semiconductors, Sendai, Japan, 19-20 December 2002

その他

2005 chair of the 2005 Gordon Research Conference on Quantum Information Science, Ventura CA, USA